ELSEVIER

Journal of Power Sources 81–82 (1999) 575–580

JOURNAL OF POWER SOURCES

www.elsevier.com/locate/jpowsour

Studies of $LiCoO_x$ thin film cathodes produced by r.f. sputtering

C.N. Polo da Fonseca [a], J. Davalos [a], M. Kleinke [a], M.C.A. Fantini [b], A. Gorenstein [a,*]

[a] *DFA / IFGW / UNICAMP, CP 6165, CEP 13084-970 Campinas, SP, Brazil*
[b] *Instituto de Fisica-USP, CP 66318, CEP 05389-970 São Paulo, SP, Brazil*

Abstract

Thin films of $LiCoO_x$ were deposited by r.f. sputtering, from a $LiCoO_2$ target and in an O_2/Ar atmosphere. The structural properties were studied by XRD and IR, the morphology by AFM and the electrochemical properties by cyclic voltammetry and galvanostatic charge/discharge techniques in 1 M $LiClO_4$/PC + EC electrolyte. As-grown films were amorphous and presented compact grain morphology. Annealing promotes a melt of the film at 300°C, followed by crystallisation at higher temperatures. The IR and XRD spectrum of films annealed in air showed the same structural reordering above 300°C. The crystalline film has been identified as a mixed $LiCoO_2 + Li_{1.47}Co_3O_4$ phase. The open circuit potential for both films is 3.45 V. The films can be cycled till ~4.2 V, but the crystalline structure presents irreversible phase changes, which limits the cyclability of the material. The films are interesting potential materials to be used at cathodes in lithium batteries.

Keywords: $LiCoO_x$; Microbatteries; Thin films

1. Introduction

Thin film microbatteries [1] have potential applications in microelectronics. It is an interesting field of research, due to the possibility of developing materials with different compositions, microstructures and morphologies.

Both binary and ternary oxide thin films have been shown to be well suited for lithium battery cathodes [2]. The ternary oxides can attain higher potentials. To the best of our knowledge, the following ternary oxides have been investigated in thin film form: Li_xCoO_2 [3,4], Li_xNiO_2 [5] and $Li_xMn_2O_4$ [6].

Different deposition techniques can be used for the production of thin films. Reactive sputtering is one of the most used techniques since it promotes the formation of homogeneous films with defined thickness. By varying the synthesis conditions, it is possible to change the composition, crystalline structure and morphology of the films. In this work, $LiCoO_x$ thin films were deposited by r.f. reactive sputtering. X-Ray Diffraction (XRD) and Infrared Spectroscopy (IR) were used to investigate the microstructure of as grown and annealed films. The morphology was studied by Atomic Force Microscopy (AFM). Electrochemical studies were performed in order to investigate the use of the films as cathodes in lithium batteries.

2. Experimental

The films were prepared by r.f. reactive sputtering, in an $O_2 + Ar$ atmosphere. The substrates were glass plates covered with a conducting SnO_2 film. The target was produced [7] by dissolving $LiOH \cdot H_2O + Co(NO_3)_2 \cdot 6H_2O$ in NH_4OH. This solution was dried under vacuum for 4 h at 60°C, and the final product was heated for 2 h at 800°C in air. The powder was then cold pressed, in the dimensions of the target. The total pressure during deposition was 7.0×10^{-3} mbar and the power was 50 W. The thickness of the films was 0.2 μm, as measured by profilometry. Films were annealed up to 600°C in air.

The X-Ray Diffraction (XRD) measurements at θ–2θ geometry were performed using Ni filtered Cu-Kα radiation. Infrared spectroscopy was performed in the transmission mode, using a JASCO IR 700 spectrophotometer. For the IR measurements, the films were deposited onto polished KBr substrates. Morphology was investigated with a Topometrics TMX 2000 Atomic Force Microscope (AFM). In this last measurements, the films were deposited onto quartz substrates.

* Corresponding author. Tel.: +55-19-7885411; Fax: +55-19-7885376; E-mail: annette@ifi.unicamp.br

0378-7753/99/$ - see front matter
PII: S0378-7753(99)00107-X

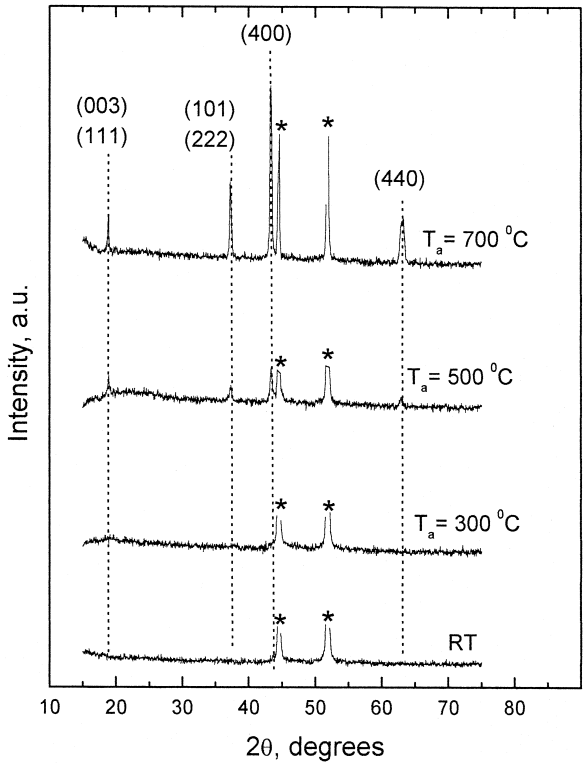

Fig. 1. X-Ray diffractograms performed on as grown film (indicated in the figure as RT), and films annealed in air. Films were deposited on Ni substrates. The diffraction peaks of the substrate are indicated in the figure by an asterisk.

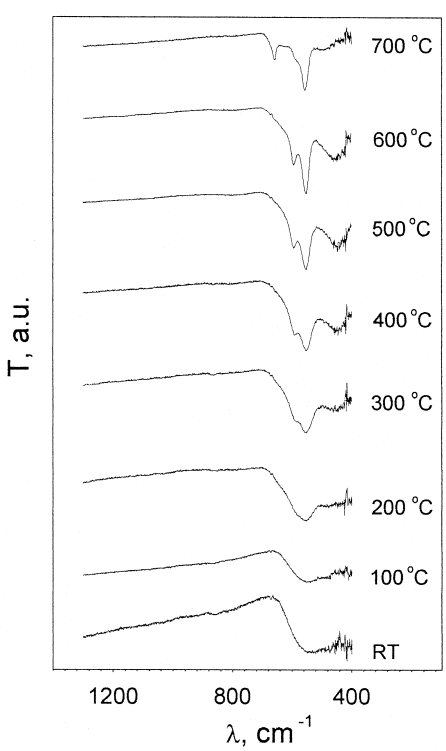

Fig. 2. IR transmittance performed on as grown film and films annealed in air from 300°C to 700°C. The substrates were KBr crystals.

The electrochemical characterisation was performed using cyclic voltammetry, chronopotentiometry and electrochemical impedance spectroscopy (EIS). The counter and reference electrodes were two lithium metal foils. The electrolyte was 1:1 ethylene carbonate (EC) and propylene carbonate (PC) solution with 1 M of $LiClO_4$. All the experiments were done with the cell in a dry box under argon. An EG&G PAR 273 potentiostat/galvanostat and a 1255 frequency response analyser (Solartron) were used.

3. Results and discussion

Fig. 1 presents the XRD results for as grown and annealed films. The XRD data indicates that the films

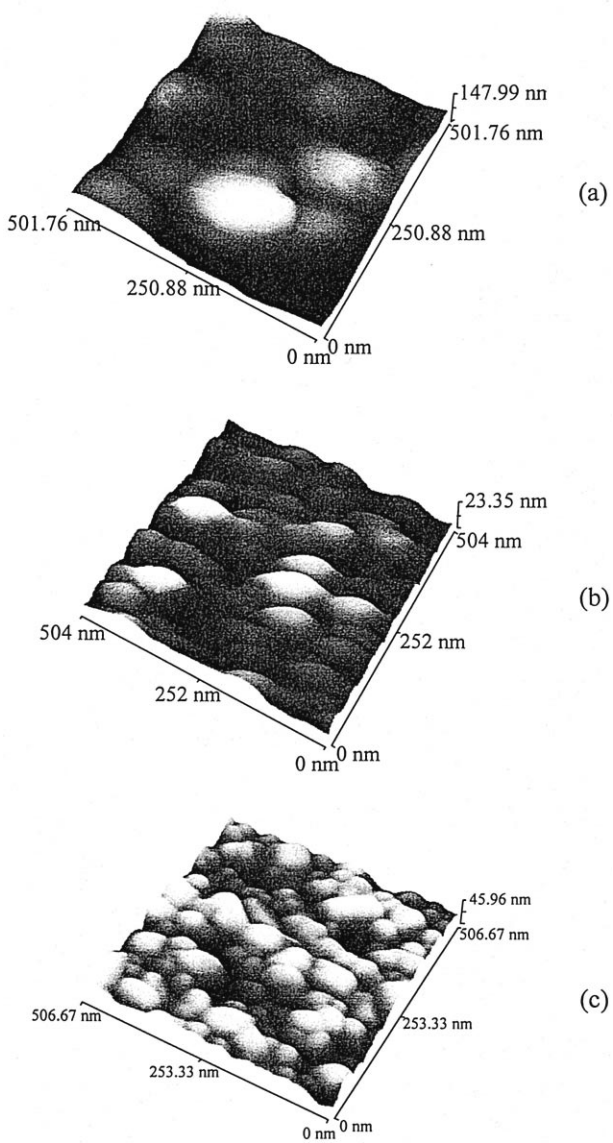

Fig. 3. AFM micrographs performed on as grown films (a), and films annealed in air at 400°C (b) and 600°C (c). Films were deposited on quartz substrates.

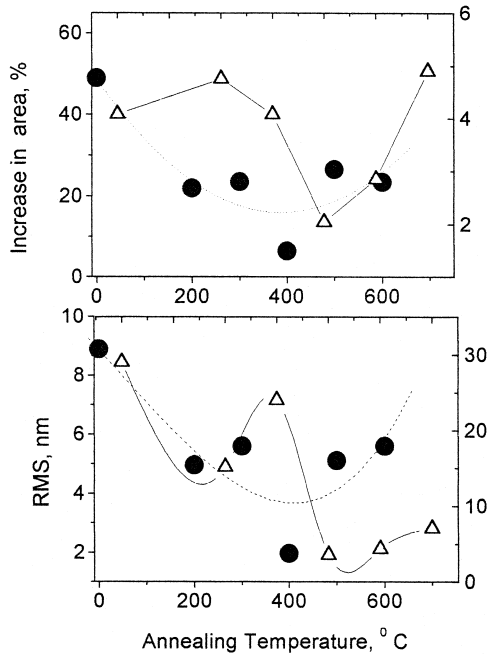

Fig. 4. Percentual increase in surface area (upper figure) and roughness (lower figure) as a function of annealing temperature.

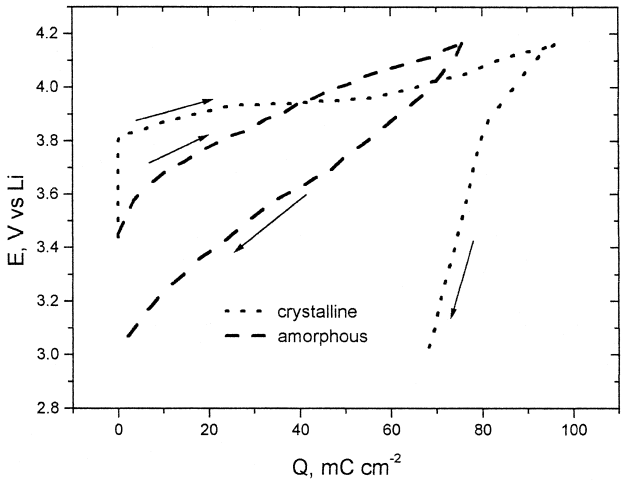

Fig. 6. Galvanostatic charge/discharge curve for crystalline and amorphous films in 1 M $LiClO_4$ /EC:PC solution. The cell was charged with 5 μA up to 4.1 V cut-off voltage and discharge with −5 μA up to 3.0 V cut-off voltage.

without any thermal treatment are amorphous. Annealing promotes crystallization, and for annealing temperatures higher than 300°C diffraction peaks can be seen in the diffractograms (Fig. 1). These diffraction peaks are located at $2\theta = 18.9°$, 37.2°, 42.3° and 63.1°. The first two peaks corresponds well with the (003) and (101) lines of $LiCoO_2$ [8]. All the measured diffraction lines has also been observed in the compound with overall composition $Li_{1.47}Co_3O_4$ [9], which has been obtained by lithium intercalation in pristine Co_3O_4. These results indicate that the annealed films can be a two-phase compound ($LiCoO_2$ + $Li_{1.47}Co_3O_4$). The results obtained by XRD were complemented with IR analysis. The IR spectra (Fig. 2) shows a broad band centered at ~560 cm^{-1} for the as-grown films. Defined peaks at 660 cm^{-1}, 595 cm^{-1}, 550 cm^{-1} and 460 cm^{-1} shows up with the increase of annealing temperature. These bands are related to the vibrational modes of Co–O, O–Co–O and Li–O in $LiCoO_2$ and has been observed both in lamellar and spinel $LiCoO_2$ phase [10,11].

Fig. 3 shows the AFM micrographs of as grown and annealed films at different temperatures. The topography of as-grown films presents large grains, with a medium

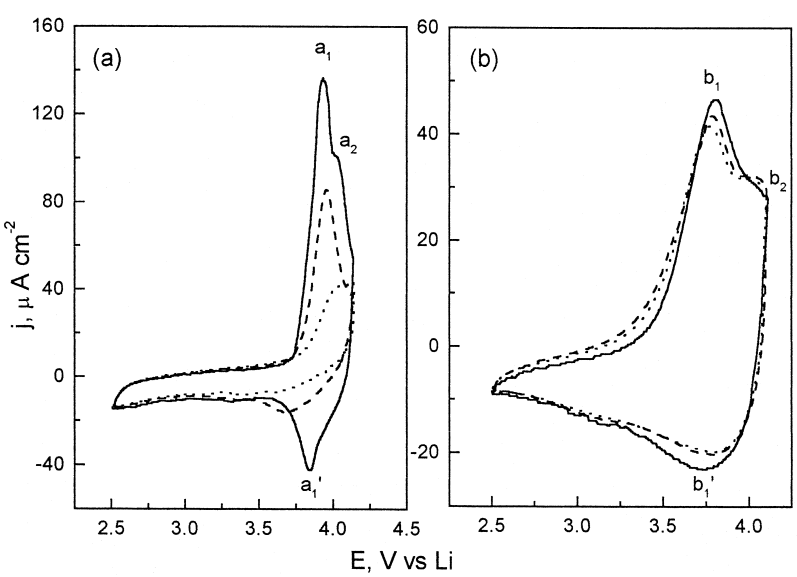

Fig. 5. Cyclic voltammograms for crystalline films (a) and amorphous films (b) in 1 M $LiClO_4$/EC:PC solution. Scan rate: 0.5 mV s^{-1}. First cycle (————), 5th (- - -); 7th (· · ·).

size of ~200 nm. The grain size decreases to ~120 nm for the annealed films. The surface area (Fig. 4), which is an important factor in electrochemical calculations, as well as the roughness decreases strongly with the increase in annealing temperature up to 400°C. For higher temperatures, an increase was observed in both parameters. The variation of surface area is 35% higher than the geometrical area for the as-grown film, and at least 10% higher for the annealed samples.

Fig. 5 presents the cyclic voltammetric profiles of crystalline (Fig. 5a) and amorphous (Fig. 5b) films. The crystalline films presented, for the first cycle, well defined anodic/cathodic peaks (Li intercalation/deintercalation process), with peak potentials located at 3.93/3.85 V

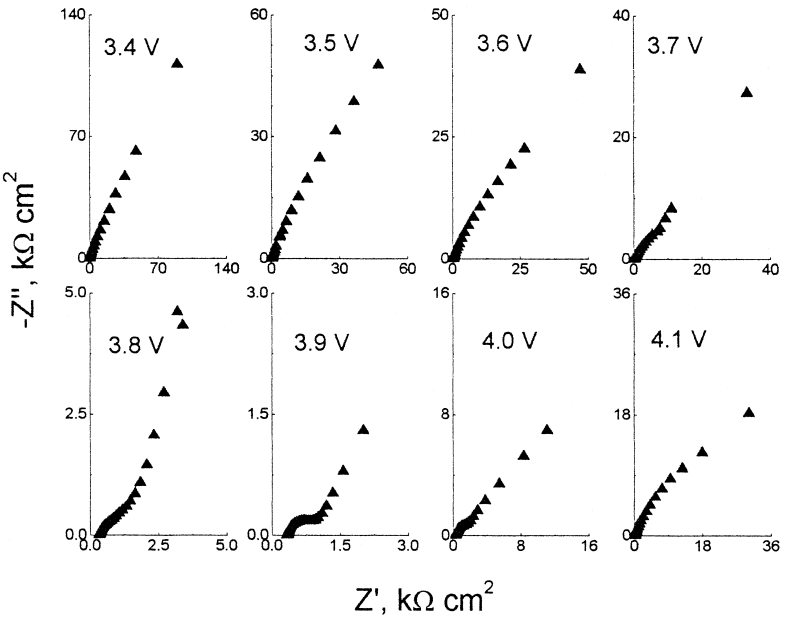

(a)

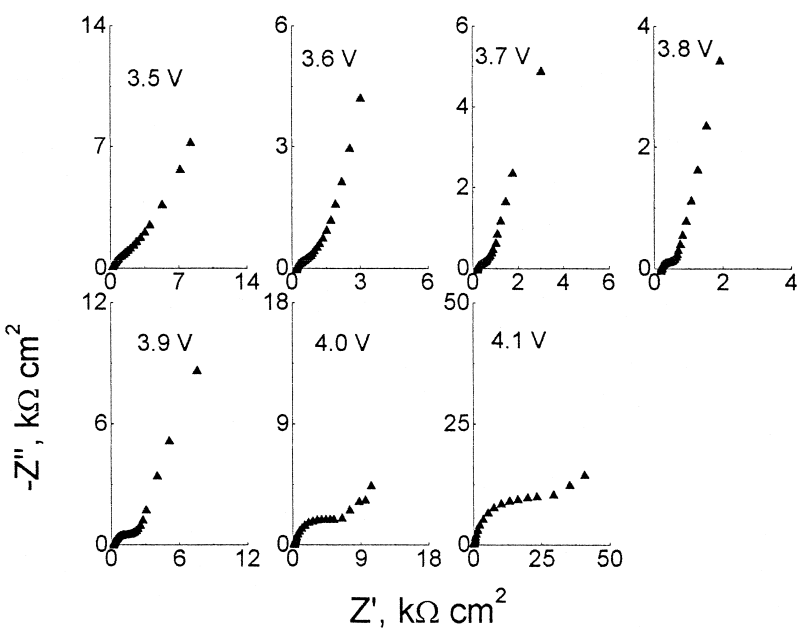

(b)

Fig. 7. Nyquist plots for crystalline (a) and amorphous (b) films polarized at different potentials. Perturbation amplitude: 0.01 V. Frequency range: 10^{-3} to 10^{5} Hz.

(a_1/a'_1 peaks, Fig. 5a). The corresponding peaks of amorphous films are broader, and the anodic/cathodic peak potentials are located at 3.80/3.75 V (b_1/b'_1 peaks, Fig. 5b). Also, a less pronounced peak, located at 4.04 V, is observed for both films (a_2 and b_2, Fig. 5a and b). This peak has been already observed by other authors [12], and it has been attributed to order/disorder phase transitions.

On continuously cycling, the crystalline film shows a great loss of electrochemical activity; the anodic/cathodic charge at the seventh cycle is ~60% less than for the first cycle. On the other hand, the amorphous film does not present great variations with cycling (≈10.6%). The loss in the load capacity and the increase of the electric resistance after several cycles has been attributed to the degradation of the electrolyte and/or the degradation of the cathode, since the total removal of lithium from the Li_xCoO_2 film promotes the oxidation of the Co^{+3} to Co^{+4}, forming an unstable phase [13].

Fig. 6 presents the galvanostatic charge/discharge plots for the amorphous and crystalline thin films electrodes. The initial open circuit potential is 3.45 V for both films. The charging process was limited to a 4.15 V cut-off potential, due to electrolyte stability limitations. The amorphous film presents an S-shaped charge/discharge curve, characteristic of a one-phase process (Fig. 6a). The de-inserted charge is 76 mC cm^{-2}, which is equivalent (if a $LiCoO_2$ composition is assumed for the as-grown film) to a composition $Li_{0.85}CoO_2$ at the end of the charging cycle. All the de-inserted lithium can be re-inserted on discharging. In the case of the crystalline film a wide plateau near 3.95 V is observed (Fig. 6b). The occurrence of this plateau indicates a phase transition, which has been attributed to phase transitions between two hexagonal structures with different unit cell c parameter [13]. The de-inserted charge is 95 mC cm^{-2}, which is equivalent to a composition $Li_{0.81}CoO_2$ at the end of the charging cycle. In the discharging cycle, however, only 30% of this charge can be re-inserted, probably due to the (irreversible) phase transitions observed in the charging process.

The impedance spectra of as grown and annealed films are shown in Fig. 7a (crystalline films) and Fig. 7b (amorphous films). In these experiments, the potential indicated in each spectrum was applied till the current was less than 0.1 μA. In the high frequency range, the first intersection of the graph with the real axis corresponds to the resistance of the electrolyte (300 Ω cm^2). The semicircle (not very well defined) at medium frequencies corresponds to the charge transfer process; also, the diffusion process can be acting in this frequency range. At low frequencies, a straight line inclined at 45° characterises the diffusion process. The charge accumulation process, characterised by a straight vertical line, is observed, at low frequencies, in some spectrum.

A drastic decrease in the charge transfer resistance (Fig. 8) is observed for films polarised at potentials in the range 3.5 to 3.8 (amorphous films) or 3.4 to 3.9 V (crystalline films); the resistance increases again for potentials in the 3.9 to 4.1 V range (amorphous films) or 4.0 to 4.1 V range (crystalline films). The resistance decrease (conductivity increase) is closely related to the process of lithium extraction. The minimum of resistance (Fig. 8) occurs for films polarised at the same potential of the main anodic peaks (a_1 and b_1, Fig. 5a and b). Other authors [14,15] have also observed the same conductivity variation, and have attributed these changes to modifications in the crystalline structure of the material.

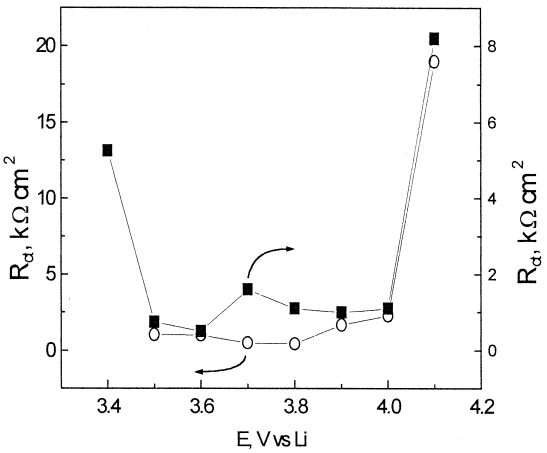

Fig. 8. Charge transfer resistance for crystalline (■) and amorphous (○) films polarized at different potentials.

4. Conclusions

In this work, $LiCoO_x$ thin films were deposited by r.f. reactive sputtering. The as-grown films were amorphous, and the crystalline film, obtained by annealing, is a mixed $LiCoO_2 + Li_{1.47}Co_3O_4$ phase. The open circuit potential for both films is 3.45 V. The films can be cycled till ~4.2 V, but the crystalline structure presents irreversible phase changes, which limits the cyclability of the material. The films are interesting potential materials to be used at cathodes in lithium batteries.

Acknowledgements

FAPESP and CNPq provided financial support.

References

[1] C. Julien, G.A. Nazri, Solid-State Batteries, Kluwer Academic Pub., MA, USA, 1994.
[2] C. Julien, Solid state batteries, in: P.J. Gellings, H.J.M. Bouwmeester (Eds.), CRC Handbook of Solid State Electrochemistry, CRC Press, NY, 1997.
[3] B. Wang, J.B. Bates, F.X. Hart, B.C. Sales, R.A. Zuhr, J.D. Robertson, J. Electrochem. Soc. 143 (10) (1996) .
[4] P. Fragnaud, T. Brousse, D.M. Schleich, J. Power Sources 63 (1996) 187.

[5] M. Yoshimura, K.S. Han, S. Tsurimoto, Solid State Ionics 106 (1998) 39.
[6] F.K. Shokoohi, J.M. Tarascon, B.J. Wolkens, D. Guyomard, C.C. Chang, J. Electrochem. Soc. 137 (1992) 1845.
[7] D. Courant, N. Baffier, B. García, J.P. Pereira-Ramos, Solid State Ionics 91 (1996) 45.
[8] Power Diffraction File Inorganic Phases Search Manual (Hanawalt) JCPDS. Published by the International Center for Diffraction Data (ICDD), USA.
[9] M.M. Thackeray, S.D. Baker, K.T. Adendorf, J.B. Goodenough, Solid State Ionics 17 (1985) 175.
[10] E. Zhecheva, R. Stoyanova, M. Gorova, R. Alcántara, J. Morales, J.L. Tirado, Chem. Mater. 8 (7) (1996) 1429.
[11] W. Huang, R. Frech, Solid State Ionics 86–87 (1996) 395.
[12] M. Antaya, K. Cearns, J.S. Preston, J.N. Reimers, J.R. Dahn, J. Appl. Phys. 76 (5) (1996) 2799.
[13] J.N. Reimers, J.R. Dahn, J. Electrochem. Soc. 139 (8) (1992) 2091.
[14] M. Shibuya, T. Nishina, T. Matsue, I. Uchida, J. Electrochem. Soc. 143 (1996) 3157.
[15] H. Sato, D. Takahashi, T. Nishina, I. Uchida, J. Power Sources 68 (1997) 540.